Catal Lett (2008) 125:169–176
DOI 10.1007/s10562-008-9567-5

Gold-Catalyzed Aerobic Oxidation of Benzyl Alcohol: Effect of Gold Particle Size on Activity and Selectivity in Different Solvents

Peter Haider · Bertram Kimmerle · Frank Krumeich · Wolfgang Kleist · Jan-Dierk Grunwaldt · Alfons Baiker

Received: 22 May 2008 / Accepted: 27 June 2008 / Published online: 16 July 2008

Abstract The effect of the size of gold particles deposited on CeO_2 and TiO_2 supports on their catalytic behavior in the aerobic oxidation of benzyl alcohol in different solvents (mesitylene, toluene, and supercritical carbon dioxide) has been investigated. The size of supported gold particles deposited via a colloidal route was in the range 1.3–11.3 nm, as determined by means of EXAFS and HAADF-STEM measurements. The catalytic performance of the supported gold catalysts in the different solvents revealed a significant effect of the gold particle size. Optimal activity was observed for catalysts with medium particle size (ca. 6.9 nm) whereas smaller and bigger particles showed inferior activity. Identical trends for the activity–particle size relationship were found using Au/CeO_2 and Au/TiO_2 for the reaction at atmospheric pressure in conventional solvents (mesitylene, toluene) as well as under supercritical conditions ($scCO_2$). Selectivity to benzaldehyde was only weakly affected by the gold particle size and mainly depended on reaction conditions. In supercritical CO_2 ($scCO_2$) selectivity was higher than in the conventional solvents under atmospheric pressure. All catalysts tested with particle sizes ranging from 1.3 to 11.3 nm showed excellent selectivity of 99% or higher under supercritical conditions.

P. Haider · B. Kimmerle · F. Krumeich · W. Kleist · J.-D. Grunwaldt · A. Baiker (✉)
Department of Chemistry and Applied Biosciences, ETH Zürich, Hönggerberg, HCI, 8093 Zurich, Switzerland
e-mail: baiker@chem.ethz.ch

Present Address:
J.-D. Grunwaldt
Department of Chemical and Bioengineering, Technical University of Denmark, 2800 Lyngby, Denmark

Keywords Gold catalyst · Particle size effect · Benzyl alcohol · Aerobic oxidation · Supercritical CO_2 · Gold colloids

1 Introduction

Gold (nano-) particles—larger colloids are often referred to as Purple of Cassius—are known and used for centuries [1] and various recipes have been described, e.g., in Libavius' chemistry book "Alchemia" published in 1597 [2]. Faraday described in one of his lectures a dependence of the color of the Au particles on the concentration of the original solution [3] addressing a today well-known and well-described [4, 5] change in color for different particle diameters of Au [6]. Various recipes for the preparation of gold colloids are known [6–11] and Au colloids are applied in various fields [12].

Triggered by its unprecedented catalytic properties gold has also attracted tremendous interest in the past years in both heterogeneous and homogeneous catalysis [13]. Due to several complicating factors caused by the application of different catalyst precursors, preparation routes, and pretreatments the assessment of particle size effects is often not straightforward. It seems crucial for the elucidation of the particle size effect to employ only one preparation method as important variables such as impurities, remaining residues on the catalysts surface, and particle morphology might be altered by using different preparation techniques [7, 14]. Also a change of the support [15] or a foreign atom [16] can affect the morphology of adsorbed Au particles which directly influences the binding energy of oxygen [17].

The presence or absence of certain low-coordinated sites like B_5 sites, edges, kinks, steps, corner atoms and also

metal facets can strongly affect the reaction pathway of a heterogeneously catalyzed reaction [18–23]. Different facets or the different (relative or absolute) amounts of low coordinated atoms as a result of a different particle size lead to different activities and selectivities, e.g., in hydrogenation reactions on Au catalysts [24, 25] and other selective oxidations [26, 27]. Hence, an optimum for activity and/or selectivity for certain reactions is found at larger particle diameters while other reactions show superior performance at smaller particle diameters. Also the shape and symmetry of the particle itself influences the site population and geometry [28–32].

It has been shown both experimentally and theoretically that the activity of Au nanoparticles in the oxidation of CO increases with decreasing particle size and is strongly affected by (defect sites in) the support [33–42]. However, bulk Au has been employed in certain oxidation reactions as well [43–45] indicating that also the presence of larger Au particles can be favorable.

Here we elucidate the effect of the gold particle size of titania and ceria-supported gold catalysts used in the aerobic oxidation of benzyl alcohol at atmospheric pressure in conventional solvents as well as at high pressure in supercritical CO_2 which can act as a (weak) Lewis base [46–51]. The almost gas-like diffusion coefficients of solutes in dense carbon dioxide and the avoidance of phase boundaries under single-phase conditions in combination with its ability to solvate nonpolar gases as well as many organic compounds render it a promising reaction medium [52–55].

2 Experimental

2.1 Catalyst Preparation

Au/TiO_2 and Au/CeO_2 catalysts were prepared by modifying a recipe previously published by our group [6, 56]. In this preparation route, Au particles are synthesized by the addition of the Au precursor (generally a solution of 1 g $H[AuCl_4]$ or $H[AuCl_4] \times 3H_2O$ in 100 mL H_2O) to a vigorously stirred alkaline solution of the reducing agent tetrakis(hydroxymethyl)phosphonium chloride (THPC). Subsequently, the colloids are immobilized on TiO_2 or CeO_2. It has been shown recently that both oxides are suitable support materials for Au catalysts [57, 58]. To fine-tune the particle size of the colloids obtained, different ratios of the reducing agent THPC and the Au precursor have been employed. In the original publication, 10 mg Au colloid have been synthesized in 50 mL deionized water using an equimolar ratio of THPC and Au. Furthermore, colloids have been prepared using a ratio THPC/Au of 4 (resulting in a mean diameter of 1.3 nm) and a ratio of 0.8 (mean particle diameter 6.9 nm). Larger particles (mean diameter 11.3 nm) were prepared by addition of 1 mL of the $H[AuCl_4]$ solution and a stoichiometric amount of THPC to the original colloidal suspension. Note that in *all* alterations of the original recipe, the molar ratio NaOH/(THPC + Au) of three was used for the preparation of the colloids except for the smallest particles (mean diameter 1.3 nm) where a ratio of six was used. All catalysts prepared exhibit a gold loading of 0.5–0.8 wt.% as evidenced by means of AAS, the values obtained for catalytic activity were corrected for the Au loading. The Tammann temperature ($0.5\ T_{melt}(Au)$) and Hüttig temperature ($0.3\ T_{melt}(Au)$) were calculated according [59].

2.2 Catalytic Testing

All catalysts were tested at atmospheric pressure similar to [57] in mesitylene (Arcos Organics, 99%, extra pure) or toluene (Fluka, purity > 99.7%) and under pressurized conditions using CO_2 as solvent. The reaction under atmospheric pressure was performed at 100 °C in a 50 mL 2-neck round bottom flask; an amount of 100 mg of the catalyst material was suspended in 2 mL mesitylene or toluene and 7 mmol of benzyl alcohol was added leading to a substrate/Au molar ratio of ≈1350. A cooler was placed on top to avoid fatal loss of material, the average error of the mass balance in the system was 2.01 ± 1.59%. Oxygen (PanGas, 5.0) was bubbled through the vigorously stirred (1500 rpm) liquid at a mass flow controller regulated stream of 50 mL/min. Tetradecane was employed as an internal standard. Samples were taken at the beginning and during the reaction and analyzed by means of gas chromatography (Thermo Quest Trace 2000; HP-FFAP capillary column; FID detector).

The high-pressure batch reactor experiments were conducted in a 100 mL autoclave made of Hastelloy B (Premex Reactor AG, Lengnau). The alcohol (7 mmol) and the powdered catalyst (100 mg) were put in the reactor, which was then closed and linked to the gas lines. Oxygen (99.5%) was added at room temperature until a pressure of 3.4 bar was reached and subsequently 30 g or 70 g of CO_2 were added, yielding a pressure at 100 °C of 90 bar and 147 bar, respectively. While a biphasic system was existent at 90 bar, a single, supercritical phase was formed at 147 bar [55]. At the end of the reaction, samples were taken by dissolving the reactor contents in 50 mL toluene (Fluka, puriss. p.a.). After filtration of the catalyst, the reaction mixture was injected in a gas chromatograph (HP 6800 series) equipped with FID detector and HP5 GC column (Agilent Technologies Inc).

Under the chosen GC variables the detection of benzyl benzoate was possible even at high selectivity values close to 100%. The relative standard deviation among the different experiments with respect to selectivity was found to

be below 5%, the standard deviation with respect to activity was smaller than 7.5%. The turnover frequency was calculated based on the number of surface Au atoms which was determined using the particle diameter determined by means of electron microscopy, assuming spherical particles and taking the total spherical surface into account according to $A = 4\pi r^2$, or, in other words, assuming an "aurophobic" surface with a critical angle of 180°. Hence, the calculations lead to the maximum surface for a spherical shape under the given value for the particle diameter and represent thus conservative estimates. All values were determined after a reaction time of 3 h.

2.3 Electron Microscopy

Samples were collected instantaneously after the preparation of the Au colloids and subsequently analyzed to minimize perturbing effects occurring with time like agglomeration or particle growth. The microscope (Tecnai F30 FEI, with a field emission cathode, operating at 300 keV, with a point resolution of <2 Å) was also equipped with a high-angle annular dark field (HAADF) detector for scanning transmission electron microscopy (STEM), and an energy-dispersive X-ray (EDX) detector. This instrumentation is capable of detecting even very small metal particles (<1 nm) by Z contrast and of analyzing selected points by EDX spectroscopy. Note that the gray fog on some of the STEM pictures derives from a larger thickness of the carbon foil used as support. For determination of the mean diameter, *all* STEM pictures recorded were taken into consideration.

2.4 XPS Measurements

XPS analysis of the Au/TiO_2 catalysts was performed on a Leybold Heraeus LHS11 MCD instrument using Mg K_α (1253.6 eV) radiation. The sample was pressed into a sample holder, evacuated in a load lock to 10^{-6} mbar, and transferred to the analysis chamber (typical pressure $<10^{-9}$ mbar). The peaks were energy-shifted to the binding energy of Ti $2p_{3/2}$ for TiO_2 (458.5 eV) to correct for the charging of the material. The surface composition of the catalysts was determined from the peak areas of Au 4*f*, Ti 2*p*, O 1*s*, N 1*s*, S 1*s* and C 1*s*, which were computed after subtraction of the Shirley-type background by empirically derived cross section factors. The relative error of the analysis was ±5%. The binding energies of metallic Au nanoparticles were determined by peak fitting.

2.5 EXAFS Measurements

EXAFS spectra were recorded at the synchrotron facility ANKA (Forschungszentrum Karlsruhe; 2.5 GeV; 130 mA injection current; ANKA-XAS beamline) using a Si(111) double-crystal monochromator detuned to about 60% of the maximum intensity. An ionization chamber was used to determine the incoming X-ray intensity. EXAFS spectra for Au/TiO_2 were recorded in fluorescence and transmission mode whereas spectra for Au/CeO_2 were only recorded in fluorescence mode. A five-element Ge solid-state detector (Canberra) was applied to measure the Au L_α fluorescence of Au (fluorescence window from 9.60 to 9.75 keV; excitation at Au L_3, 11.919 keV). For this purpose, the sample was pressed as a pellet and positioned in a 45° angle in the beam [60]. Extraction of the EXAFS function and data analysis was performed using Athena 0.8.049 [61]. Fourier transformed EXAFS spectra were calculated applying Fourier transformation on the k^3-weighted functions typically in a k-range of 2.5–12 $Å^{-1}$ for Au/TiO_2 and 2.5–8 $Å^{-1}$ for Au/CeO_2 samples.

3 Results and Discussion

Au colloids of four different sizes (mean diameters: 1.3, 2.1, 6.9, and 11.3 nm) were prepared by reduction of $H[AuCl_4]$ by tetrakis(hydroxymethyl)phosphonium chloride (THPC) in alkaline solution. Only this preparation route was used to prepare the Au colloids, the particle diameter was controlled by adjusting the ratio of THPC and Au in the preparation procedure. A simple temperature treatment of the catalysts aiming at creating larger particles was not considered as a useful strategy due to the multiple effects of such a treatment on the Au particles. A thermal treatment above the Hüttig (≈128 °C) or even Tammann (≈396 °C) temperature [59] does not only affect the particle size but probably also alters the particle morphology and changes the amount of defects, edge and corner atoms or exposed crystal surfaces hence possibly affecting the catalytic performance and making it impossible to derive conclusions exclusively related to the Au particle size.

The STEM images of three of the prepared colloids, which are depicted in Fig. 1, show a homogeneous distribution of the Au particles in solution. The smallest particles produced (Fig. 1a and b) possess a mean diameter of only 1.3 nm (at a standard deviation of 0.5 nm). Note that there are a few larger particles in Fig. 1 a and b exhibiting a size of up to 3 nm that somewhat differ from the neighboring small nano- and subnanoparticles. However, these larger particles are too few in number to cause a more severe distortion of the particle size distribution. Fig. 1c and d represents the colloids prepared by the "standard" recipe [6, 56] and also exhibit a very homogeneous size distribution (mean particle size 2.1 nm, standard deviation 0.7 nm). Immobilization of these colloids on TiO_2 and CeO_2 was also studied by means of

STEM to verify the size of the particles after the immobilization on the support (for STEM images of this catalyst consult references [55, 62]). The selection of the support is critical as different materials exhibit different "aurophilicities," hence the adsorption of an identical colloid can lead to a strong deviation in the final particle size obtained due to a higher or lower critical contact angle with the support [55]. Also after immobilization, agglomerated particles were only detected to a minor amount and the determination of the mean particle size lead to similar values as obtained for the Au colloids in solution (mean particle size = 2.0 nm, standard deviation 0.6 nm), corresponding TEM/STEM images are presented in [55, 56]. However, the synthesis of larger Au particles was somewhat more difficult as the particle size distribution was found to broaden significantly when the Au concentration in the original recipe was increased keeping the other concentrations constant. THPC as a reducing agent is only strong enough to reduce the Au precursor in alkaline solution [6, 63, 64] according to

$$P(CH_2OH)_4^+ + OH^- \rightarrow P(CH_2OH)_3 + HCHO + H_2O$$

This reatcion is followed by the subsequent formation of tris(hydroxmethyl)phosphonium oxide (THPO)

$$P(CH_2OH)_3 + H_2O \rightarrow OP(CH_2OH)_3 + H_2$$

A further reaction in alkaline solution leads to the formation of bis(hydroxymethyl)phosphinic acid [63]:

$$OP(CH_2OH)_3 + H_2O \xrightarrow{[OH^-]} (CH_2OH)_2P(O)OH + H_2 + HCHO$$

Hence, the pH-value in the solution plays a vital role for the redox-behavior of THPC. It is thus assumed that an increase of the Au concentration or rather the concentration of $H[AuCl_4]$ (tetrachloroauric acid), in solution alters the pH conditions in an unfavorable way leading to the formation of large and agglomerated particles. We presume that in the case of a low pH, the redox capabilities of THPC are not sufficient and hence, the size of the particles is probably not only influenced by the reduction step but also crystallite growth or agglomeration starts to play a role. As the molar ratio of (NaOH + THPC)/Au was set to a value of three in the original recipe, this value was taken as a minimum for all further preparations of Au colloids. An increase of this ratio up to a value of six by increasing the amount of NaOH did not negatively affect the size of the Au colloids nor broaden the particle size distribution. The colloids exhibiting a mean diameter of 6.9 nm are depicted in Fig. 1e and f. Histograms of all the particles synthesized and subsequently used in the aerobic oxidation of benzyl alcohol are presented in Fig. 2, and the results of a statistical evaluation of the particle size distribution are given in Table 1.

The results obtained from STEM pictures were correlated with EXAFS measurements. The EXAFS spectra of the supported Au particles show a similar trend as already observed with STEM pictures for the colloids in solution—the Au–Au coordination number increases with increasing colloid size for Au/TiO_2 (Fig. 3a) and Au/CeO_2 (Fig. 3b). For the Au colloids exhibiting a diameter of only 1.3 nm in liquid phase, a very low Au–Au contribution is detected. This is due to the fact that the average coordination number of gold neighbors is significantly lower than 12 due to the dominance of surface gold atoms. The Au backscattering contribution in the first nearest neighbor shell ($R = 2.8$ Å) increases monotonically and it is observed that particles having a diameter of 6.9 nm still exhibit a strongly diminished Au–Au contribution with respect to the Au foil included in the graph. This is probably due to the fact that the particles are not spherically shaped. However, the largest particles analyzed here ($d_{average} = 11.3$ nm) show, as expected, a similar spectrum compared to bulk gold due to the dominance of fully coordinated gold atoms (CN = 12). Nevertheless, they still exhibit some catalytic activity in the aerobic oxidation of benzyl alcohol, probably due to the higher number of gold surface atoms compared to bulk gold. Finally, it should be noted that in all cases metallic gold was found.

XPS measurements were performed to exclude the possibility that the different catalytic activity which is attributed only to the size effect of the Au nanoparticles described in this paper could also be explained by surface impurities which might have been introduced during the preparation process. During the synthetic procedure chemicals were used that consist (aside from Ti, O, and Au) of the elements H, Cl, S, P, C, and Na. The focus of the analysis was the determination of the surface concentration of the possible contaminants, especially Na as the aerobic oxidation of alcohols is generally promoted by basic components [65]. XPS spectra of the different Au/TiO_2 catalysts and pure TiO_2 reference samples were recorded in the energy range from 1100 to 0 eV and showed only peaks that could be assigned to the elements Ti, O, Au, C, N and trace amounts of S (see Table 2). The samples analyzed showed quite similar composition of the surface. In order to verify the origin of the detected impurities, TiO_2 was analyzed "as received" (untreated TiO_2) and after a preparation treatment that was performed without the addition of Au (treated TiO_2, Table 2). Other elements (esp. Na and P) could not be observed in significant amount on the surface. Binding energies for Ti and O are in good accordance to literature data reported for TiO_2. Binding energies for the $Au_{7/2}$ and $Au_{5/2}$ peaks at 83.5 and 87.2 eV can be assigned to metallic Au nanoparticles. C and N impurities are also found in the reference TiO_2 samples and can be explained by organic residues. The small signal arising

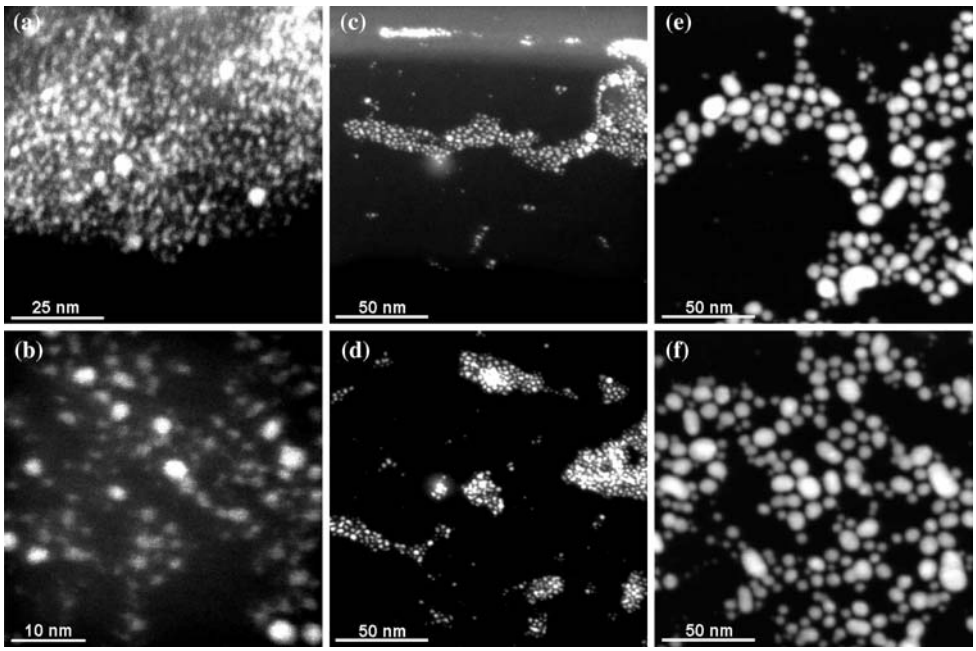

Fig. 1 Typical HAADF-STEM pictures of three different colloids: (**a**, **b**) Depict colloids showing a mean diameter of 1.3 nm, (**c**, **d**) colloid with mean diameter of 2.1 nm, (**e**, **f**) colloid with mean diameter of 6.9 nm. Note that due to the *Z*-contrast, Au particles appear as bright spots

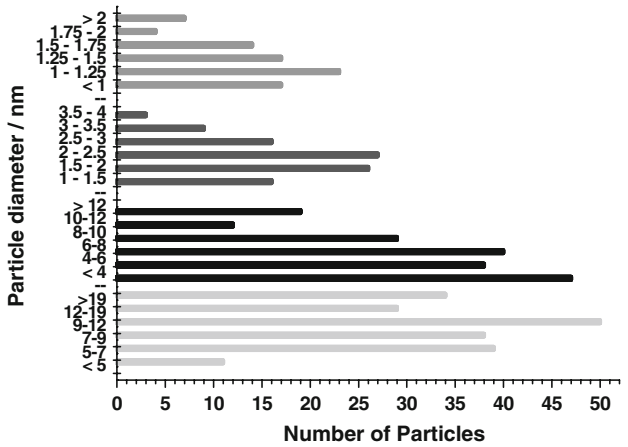

Fig. 2 Histograms compiled for the different colloids prepared. The colloids described here—from bottom to top—show a mean diameter of 11.3 nm (*black*), 6.3 nm (*light gray*), 2.1 nm (*gray*), and 1.3 nm (*dark gray*)

Table 1 Statistical evaluation of the colloids prepared, the values for average diameter, median diameter, standard deviation and skewness are reported for the four different colloids used in this study

	Col 1.3 nm	Col 2.1 nm	Col 6.9 nm	Col 11.3 nm
Number	82	97	193	201
Average	1.32	2.09	6.93	11.32
Median	1.30	2.00	6.30	9.07
St. dev.	0.47	0.68	3.61	5.95
Skewness	1.82	0.41	0.69	0.79

from sulfur was not present in the neat support. These findings strongly indicate that for an assessment of a potential effect caused by a variation in the particle size, the corresponding samples need to be prepared with a single preparation route only.

The catalytic tests of the different supported gold catalysts in the aerobic oxidation of benzyl alcohol were conducted with the as-prepared samples (Fig. 4). The results indicate that the activity is strongly influenced by the particle size, whereas selectivity shows only weak dependence on this parameter and is mainly dominated by the reaction conditions. Strikingly, the selectivity to benzaldehyde of the catalyst under high pressure (Fig. 4c and d) was superior to that observed at ambient conditions (Fig. 4a and b) and only very small amounts of benzylbenzoate were detected leading to high selectivity for all systems examined (Fig. 4c and d). Note that the value for selectivity changed by less than 1% under high pressure when the conditions were changed from an expanded liquid (90 bar) to a single phase system (147 bar).

In the field of alcohol oxidation, recent studies on unsupported gold particles [66, 67] show an increase in activity for lower Au particle size, whereas for carbon-supported Au particles [68] larger gold particles were found to be favorable for activity. In contrast to findings for unsupported Au particles and the results described in detail in the literature for the oxidation of CO [33–42], our experiments indicate that the activity increases with increasing particle size reaching an optimum at about 6.9 nm. This observation is found independently of the conditions applied and is observed under ambient pressure in different solvents (mesitylene, toluene) as well as under supercritical conditions. The conversion plotted in Fig. 4 is only normalized to similar amounts of Au, *not* to the Au particle size or the surface atoms, hence the increase in

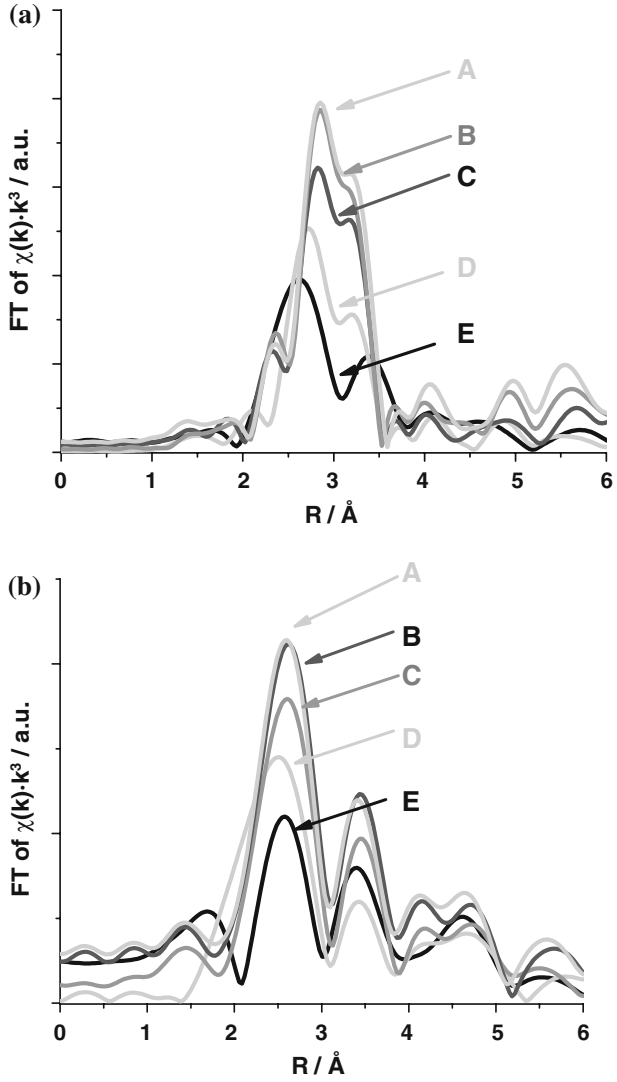

Fig. 3 Fourier transformed EXAFS spectra (k^3-weighted $\chi(k)$ function) recorded for the colloids of different size prepared and immobilized on two metal oxide supports: (**a**) Au on TiO_2; E: 1.3 nm, D: 2.1 nm, C: 6.9 nm, B: 11.3 nm, A: spectrum gold foil for comparison; note that the k-range for E was only 2.5–8 $Å^{-1}$ (**b**) Au on CeO_2; E: 1.3 nm, D: 2.1 nm, C: 6.9 nm B: 11.3 nm, A: gold foil for comparison

Table 2 XPS analyses of supported gold colloids and titania support

Element	Ti	O	Au		C	N	S
Peak	$2p_{3/2}$	1 s	$4f_{7/2}$	$4f_{5/2}$	1*s*	1*s*	2*s*
TiO_2 untreated							
Position	458.5	529.8	–	–	284.6	399.8	–
Atom %	23.3	72.0	–		4.0	0.7	–
TiO_2 treated							
Position	458.5	529.8	–	–	284.8	400.1	225.4
Atom %	22.2	70.2	–		5.3	1.5	0.8
Colloid 6.9 nm							
Position	458.5	529.7	83.5	87.2	284.8	399.9	225.3
Atom %	22.4	70.7	0.2		4.4	1.7	0.7
Colloid 2.1 nm							
Position	458.5	529.7	83.3	87.0	284.5	399.6	225.4
Atom %	22.6	70.8	0.3		5.2	1.1	tr.

Untreated TiO_2 refers to the support that was analyzed as received, treated TiO_2 represents a sample that was subjected to the preparation treatment (see Experimental section) but no Au was added. The samples colloid 2.1 and 6.9 nm refer to the supported colloids of that size

activity with increasing particle size is even more pronounced when, e.g., only the surface atoms are taken into consideration. In case of Au/CeO_2 in supercritical CO_2 (Fig. 4d), the TOF would then not only increase from 81 h^{-1} (mean diameter 2.1 nm) to 99 h^{-1} (mean diameter 6.9 nm) when taking the total number of Au into account but increase from 376 h^{-1} (mean diameter 2.1 nm) to 1244 h^{-1} (mean diameter 6.9 nm). Note that the particles exhibiting a diameter of 11.3 nm show a lower TOF value in all the cases.

Strong differences in the activity of Au/TiO_2 and Au/CeO_2 have been reported in the oxidation of alcohols under ambient pressure [57, 69]. However, the difference in activity is also found to be dependent on the conditions, e.g., the solvent, used. In mesitylene, the Au/TiO_2 exhibited a maximum conversion of only 5% under similar conditions, but with an identical dependence of catalytic activity on particle size compared to Au/CeO_2. Note that this difference in activity is far less pronounced when toluene is used as a solvent. However, also in the two regimes selected in high pressure environment (single phase and biphasic system) significant differences in the activity for the catalyst are obtained (Fig. 4c and d). In good agreement with previous results, the conversion increases in the regime of an expanded liquid [55]. The support effect is reduced and the activity is found to be larger under supercritical conditions. Generally, CO_2 is considered a Lewis acid. It has been shown that CO_2 can interact with surfaces of oxides such as TiO_2 and CeO_2 as a Lewis acid through the carbon atom and bind to a surface oxygen atom, but bond formation is also possible between the oxygen atoms and Lewis acid surface sites possibly because CO_2 exhibits also weak Lewis base properties [46–51]. Note that $scCO_2$ as the solvent is present in large excess and hence, also a weak basicity could contribute significantly to the reaction. Despite the strongly differing reaction conditions, identical behavior with respect to the dependence of catalytic activity on particle size was obtained (compare Fig. 4a and b with Fig. 4c and d). Moreover, due to the applied catalyst synthesis strategy based on the same preparation route, it is proposed that the observed effect can indeed be linked to the size of the oxide supported Au nanoparticles.

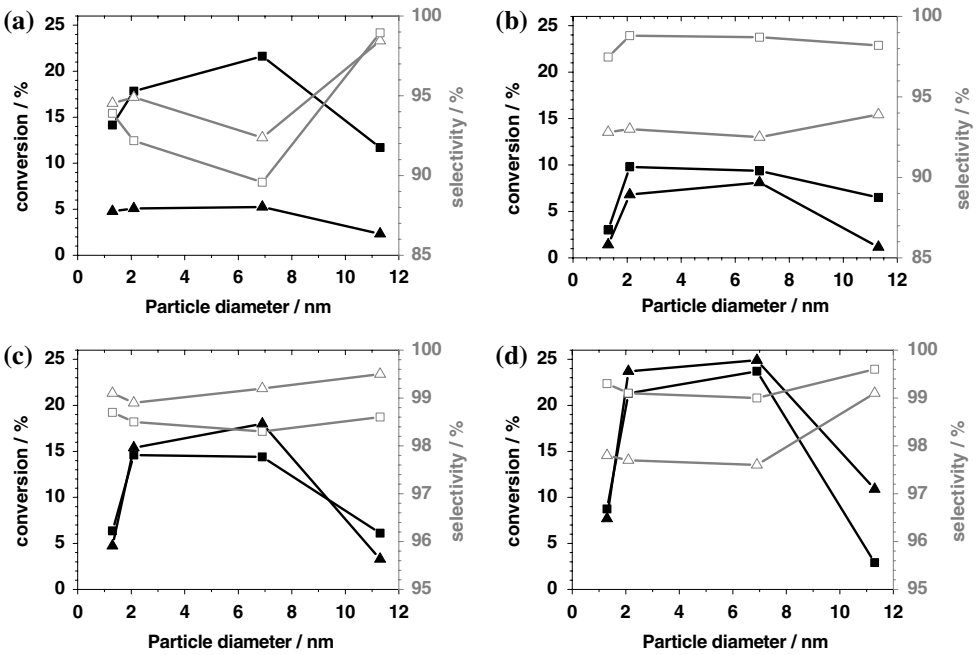

Fig. 4 Activity (*black lines*, *left axis*, *full symbols*) and selectivity (*gray lines*, *right axis*, *open symbols*) of the supported gold catalysts: Au/CeO_2 (*triangles*) and Au/TiO_2 (*squares*). The catalytic activity was evaluated under atmospheric pressure using mesitylene (**a**) and toluene (**b**) as well as under high pressure conditions ($scCO_2$) in one-phase (**c**) and two-phase (**d**) system. All values were determined after a reaction time of 3 h

4 Conclusions

We have prepared titania- and ceria-supported gold catalysts with different gold particle size in the range from 1.3 to 11.3 nm using a colloidal route. Catalytic studies of the aerobic oxidation of benzyl alcohol at atmospheric conditions in conventional solvents (mesitylene, toluene), as well as in supercritical CO_2 (one phase and two phase system depending on the applied pressure), revealed that the catalytic behavior of this reaction is affected by the gold particle size, showing highest activity for the catalyst containing gold particles of 6.9 nm average size. This behavior was observed irrespective of the support (TiO_2 or CeO_2) and of the reaction conditions applied (atmospheric pressure or supercritical conditions) and is hence attributed to the size of the Au particles.

In $scCO_2$, the formation of byproducts was strongly diminished and the selectivity at similar conversion was superior compared to that in reactions performed at atmospheric pressure in the conventional solvents. It seems that supercritical CO_2 favors the main reaction pathway under these conditions and that the support (titania, ceria) properties are less influential under these conditions.

Acknowledgements Electron microscopy was performed at the EMEZ (ETH Zurich). ANKA (Forschungszentrum Karlsruhe, Germany) is acknowledged for providing beamtime for the fluorescence XAS investigations and S. Mangold (ANKA) and S. Marx (ETH Zurich) for help and support during beamtime. The work at the synchrotron radiation source was supported by the European Community—Research Infrastructure Action under the FP6 "Structuring the European Research Area" program (through the Integrated Infrastructure Initiative "Integrating Activity on Synchrotron and Free Electron Laser Science", Contract RII3-CT-2004-506008).

References

1. Hunt LB (1976) Gold Bull 9:134
2. Libavius A (1597) Alchemia Andreae Libavii, Frankfurt, p 406
3. Faraday M (1857) Philos Trans R Soc Lond 147:145
4. Moores A, Goettmann F (2006) New J Chem 30:1121
5. Liz-Marzan LM (2006) Langmuir 22:32
6. Duff DG, Baiker A, Edwards PP (1993) Langmuir 9:2301
7. Porta F, Prati L, Rossi M, Scari G (2002) J Catal 211:464
8. Liu YL, Male KB, Bouvrette P, Luong JHT (2003) Chem Mater 15:4172
9. Shimizu T, Teranishi T, Hasegawa S, Miyake M (2003) J Phys Chem B 107:2719
10. Jorgensen JM, Erlacher K, Pedersen JS, Gothelf KV (2005) Langmuir 21:10320
11. Park J, Joo J, Kwon SG, Jang Y, Hyeon T (2007) Angew Chem Int Ed 46:4630
12. Daniel MC, Astruc D (2004) Chem Rev 104:293
13. Hashmi ASK, Hutchings GJ (2006) Angew Chem Int Ed 45:7896
14. Schubert MM, Hackenberg S, van Veen AC, Muhler M, Plzak V, Behm RJ (2001) J Catal 197:113
15. Janssens TVW, Carlsson A, Puig-Molina A, Clausen BS (2006) J Catal 240:108
16. Kiss AM, Švec M, Berkó A (2006) Surf Sci 600:3352
17. Xu Y, Mavrikakis M (2003) J Phys Chem B 107:9298
18. Somorjai GA (1976) Acc Chem Res 9:248
19. Somorjai GA, Rioux RM (2005) Catal Tod 100:201
20. Baiker A, Dollenmeier P, He R, Wokaun A (1986) J Catal 100:345
21. Baiker A, Monti D (1985) J Catal 91:361
22. Davis SM, Zaera F, Somorjai GA (1982) J Am Chem Soc 104:7453
23. Lenzsolomun P, Goodman DW (1994) Langmuir 10:172
24. Mohr C, Hofmeister H, Radnik J, Claus P (2003) J Am Chem Soc 125:1905
25. Claus P, Bruckner A, Mohr C, Hofmeister H (2000) J Am Chem Soc 122:11430
26. Lu JQ, Zhang XM, Bravo-Suarez JJ, Bando KK, Fujitani T, Oyama ST (2007) J Catal 250:350

27. Edwards JK, Solsona BE, Landon P, Carley AF, Herzing A, Kiely CJ, Hutchings GJ (2005) J Catal 236:69
28. Van Hardeveld R, Hartog F (1969) Surf Sci 15:189
29. Van Hardeveld R, Van Montfoort A (1966) Surf Sci 4:396
30. Hansen TW, Hansen PL, Dahl S, Jacobsen CJH (2002) Catal Lett 84:7
31. Jacobsen CJH, Dahl S, Hansen PL, Tornqvist E, Jensen L, Topsøe H, Prip DV, Møenshaug PB, Chorkendorff I (2000) J Mol Cat A Chem 163:19
32. Mukerjee S, McBreen J (1998) J Electroanal Chem 448:163
33. Haruta M (1997) Catal Tod 36:153
34. Haruta M, Date M (2001) Appl Cat A Gen 222:427
35. Lopez N, Janssens TVW, Clausen BS, Xu Y, Mavrikakis M, Bligaard T, Nørskov JK (2004) J Catal 223:232
36. Mavrikakis M, Stoltze P, Nørskov JK (2000) Catal Lett 64:101
37. Remediakis IN, Lopez N, Nørskov JK (2005) Appl Cat A Gen 291:13
38. Grisel R, Weststrate KJ, Gluhoi A, Nieuwenhuys BE (2002) Gold Bull 35:39
39. Bond GC, Thompson DT (2000) Gold Bull 33:41
40. Valden M, Lai X, Goodman DW (1998) Science 281:1647
41. Yoon B, Hakkinen H, Landman U, Worz AS, Antonietti JM, Abbet S, Judai K, Heiz U (2005) Science 307:403
42. Hvolbæk B, Janssens TVW, Clausen BS, Falsig H, Christensen CH, Nørskov JK (2007) Nano Tod 2:14
43. Kameoka S, Tsai AP (2008) Catal Lett 121:337
44. Xu CX, Su JX, Xu XH, Liu PP, Zhao HJ, Tian F, Ding Y (2007) J Am Chem Soc 129:42
45. Zhu BL, Angelici RJ (2006) J Am Chem Soc 128:14460
46. Raveendran P, Wallen SL (2003) J Phys Chem B 107:1473
47. Bell PW, Thote AJ, Park Y, Gupta RB, Roberts CB (2003) Ind Eng Chem Res 42:6280
48. Raveendran P, Ikushima Y, Wallen SL (2005) Acc Chem Res 38:478
49. Renault B, Cloutet E, Cramail H, Tassaing T, Besnard M (2007) J Phys Chem A 111:4181
50. Saharay M, Balasubramanian S (2006) J Phys Chem B 110:3782
51. Temtem M, Casimiro T, Santos AG, Macedo AL, Cabrita EJ, Aguiar-Ricardo A (2007) J Phys Chem B 111:1318
52. Baiker A (1999) Chem Rev 99:453
53. Grunwaldt JD, Wandeler R, Baiker A (2003) Cat Rev Sci Eng 45:1
54. Subramaniam B (2001) Appl Cat A: Gen 212:199
55. Kimmerle B, Grunwaldt JD, Baiker A (2007) Top Catal 44:285
56. Grunwaldt JD, Kiener C, Wögerbauer C, Baiker A (1999) J Catal 181:223
57. Abad A, Concepción P, Corma A, García H (2005) Angew Chem Int Ed 44:4066
58. Enache DI, Knight DW, Hutchings GJ (2005) Catal Lett 103:43
59. Trimm DL (1997) In: Ertl G, Knözinger H, Weitkamp J (eds) Handbook of heterogeneous catalysis. Wiley VCH, Weinheim, 1263 p
60. Hannemann S, Casapu M, Grunwaldt JD, Haider P, Trussel P, Baiker A, Welter E (2007) J Synch Rad 14:345
61. Ravel B, Newville M (2005) J Synch Rad 12:537
62. Grunwaldt JD, Maciejewski M, Becker OS, Fabrizioli P, Baiker A (1999) J Catal 186:458
63. Hoffman A (1930) J Am Chem Soc 52:2995
64. Vullo WJ (1968) J Org Chem 33:3665
65. Zheng NF, Stucky GD (2007) Chem Commun 37:3862
66. Tsunoyama H, Sakurai H, Tsukuda T (2006) Chem Phys Lett 429:528
67. Comotti M, Della Pina C, Matarrese R, Rossi M (2004) Angew Chem Int Ed 43:5812
68. Porta F, Prati L, Rossi M, Coluccia S, Martra G (2000) Catal Tod 61:165
69. Haider P, Baiker A (2007) J Catal 248:175